한국정밀공학회지 제 37 권 제 4 호 pp. 283-290 April 2020 / 283
J. Korean Soc. Precis. Eng., Vol. 37, No. 4, pp. 283-290 http://doi.org/10.7736/JKSPE.019.150
ISSN 1225-9071 (Print) / 2287-8769 (Online)

Advanced Film-Type Acoustic Reflector Inspired by Helmholtz Resonator

이성호[1], 최진호[1], 김규만[1,#], 노용래[1,#], 곽문규[1,#]
Sung Ho Lee[1], Jin Ho Choi[1], Gyu Man Kim[1,#], Yong Rae Roh[1,#], and Moon Kyu Kwak[1,#]

1 경북대학교 기계공학부 (School of Mechanical Engineering, Kyungpook National University)
Corresponding Authors / Email: gyuman.kim@knu.ac.kr, TEL: +82-53-950-7570, ORCID: 0000-0003-2484-2133
Email: yryong@knu.ac.kr, TEL: +82-53-950-6828, ORCID: 0000-0003-2749-199X
Email: mkkwak@knu.ac.kr, TEL: +82-53-950-5573, ORCID: 0000-0002-8902-7685

KEYWORDS: Helmholtz resonator, Acoustics, Attenuation, Roll type equipment

Sound waves propagate in a manner in which energy is transmitted by adjacent molecules in the medium. These adjacent molecules exhibit inherent sound wave characteristics, such as height and wavelength, depending on the sound frequency. The Helmholtz resonator, one of the well-known acoustic elements, comprises a neck and a cavity, and features a resonance at a specific frequency related to structural dimensions. The acoustic characteristics of the Helmholtz resonator can be explained by a lumped spring-mass system in mechanical engineering; the resonant frequency can be calculated with the same analysis. The Helmholtz resonator is widely used as an acoustic filter as it can re-radiate sound waves with the opposite phase and significantly attenuate the original sound wave in the resonance frequency range. In this study, we fabricated a Helmholtz resonator-inspired film-type acoustic absorber (FAA), comprising a microscale resonator array made with polydimethylsiloxane (PDMS). Through acoustic attenuation experiments, the FAA revealed that the novel attenuation values reached up to 36.3 dB mm-1. Additionally, a continuous fabrication of the FAA was achieved via a custom-built roll-type equipment.

Manuscript received: November 14, 2019 / Revised: January 15, 2020 / Accepted: March 4, 2020

1. Introduction

The Helmholtz resonator, comprising a neck with an open hole and a cavity with a rigid wall, exhibits resonance at a specific frequency. In several cases, an array of the Helmholtz resonators can serve as a good source of metamaterial given their simpler structure compared with other typical resonators; Helmholtz resonators present unpredictable parameter changes, such as negative pressure or negative density, at a specific resonant frequency.[1-6] The pressure in Helmholtz resonator increases when the air inside the cavity is compressed by incident sound pressure. Thereafter, the air inside the Helmholtz resonator will be released owing to the higher value of inner pressure than the outside pressure. If incident sound pressure is supplied continuously, then air flow is generated continuously. Considering this principle, the Helmholtz resonator system with continuous air flow can be considered a “spring-mass model” in mechanical engineering; thus, the Helmholtz resonator exhibits a specific resonant frequency.[7] In this spring-mass system, attenuation occurs as the incoming and outgoing signals cancel each other out. In other words, acoustic attenuation is induced by the Helmholtz resonator because the amplified and reradiated sound pressure from the Helmholtz resonator is much stronger than the incident sound pressure at resonant frequency, resulting in interference.[2,8] Considering this phenomenon, the Helmholtz resonator can be utilized as an acoustic filter.[9-11] To use the Helmholtz resonator as an acoustic filter, an easy-to-use material should be developed. As the conventional Helmholtz resonator is a large bottle type, using this equipment as an actual acoustic filter for machine parts or household goods presents difficulty. For this reason, the research on acoustic absorption and metamaterial based on the existing Helmholtz resonator will have been conducted by simulation. The size of the Helmholtz resonator must be drastically reduced to increase its usability as an acoustic filter. The Helmholtz resonator

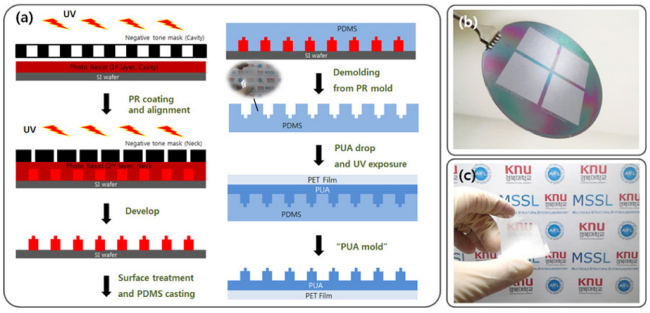

Fig. 1 (a) Schematic for SU-8 master and flexible PUA mold. (b) Photo-image of SU-8 master and (c) Photo-image of flexible PUA mold

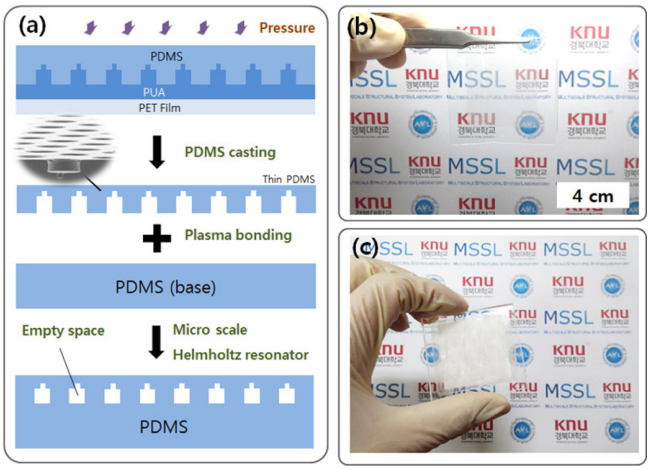

Fig. 2 (a) Schematic for fabrication flow of FAAs. (b) Photo-image for PDMS film with microresonators and (c) Photo-image of fabricated FAAs

is a simple and an admirable acoustic element; however, the fabrication of microscale Helmholtz resonator arrays features limitations.[2] Meanwhile, to apply micro/nanostructures to practical life or industrial field, numerous research groups have studied not only large-area fabrication strategies but also continuous fabrication methods. Other research groups have also exerted efforts to develop continuous fabrication systems to overcome the limitations of microelectromechanical system (MEMS) fabrication methods given the gradually increasing demands for using novel and functional materials comprising micro/nanostructures.[12-20] In this study, we present the fabrication of advanced film-type acoustic absorber (FAA) with a microscale resonator array inspired by the Helmholtz resonator. By using various MEMS fabrication methods, a large-area FAA was fabricated. The microscale resonators (0-100 μm) were arrayed easily with 184 μm period in a 40 × 40 mm square. We have conducted various experiments to determine the acoustic characteristics of the FAA. First, the performance of the FAA against ultrasonic waves was evaluated in water. By fabricating microstructures with various shapes, the relation between geometric values of the micro-Helmholtz resonator and absorption characteristic was confirmed. Furthermore, to enhance the productivity of the FAA, we have implemented its continuous fabrication by using a thermal roll-imprinting lithography system.

2. Materials and Methods

2.1 Fabrication of the Resonator Array Master Mold

Conventional photolithography and rigiflex lithography were used to prepare the Helmholtz resonator array master mold (Positive Mold) (Fig. 1). In the first step, Helmholtz resonator cavity parts were formed on a silicon wafer through the first photolithography without a development process. Neck parts were defined on the cavity-formed layer through delicate alignment of the second mask followed by the second photolithography.

During two photolithography processes, negative thick photoresist (SU-8 series, Microchem) was used, and the development process was performed at the same time. After fabrication, the mold surface was treated with a silane agent (L-SAM, Minuta Tech) for easy demolding during rigiflex lithography. To apply the fabricated mold to the roll-type equipment, a belt-type PUA mold (PUA 301RM, Minuta Tech) with the same structure as the PR mold was fabricated from the PDMS replica through rigiflex lithography (Fig. 1).

2.2 Replica Molding and Lamination of Film-Type Resonator Arrays

The PDMS fabricated in the continuous system featured a thickness of approximately 200 μm and a Helmholtz resonator structure (Fig. 2).

However, the FAA requires a support layer (Non-Patterned PDMS) to produce perfectly closed resonator structures. The FAA support layers or other FAAs were laminated using oxygen plasma treatment exposed for 2 min at 120 W in a plasma chamber (PDC-32 G, Harrick Plasma).

2.3 Acoustic Attenuation Measurement

An attenuation experiment was conducted to measure sound pressure fluctuations between the transducer and receiver in a water tank (Fig. 3). Two transducers, namely, the transmitter and receiver, were located in either side of the water tank. Thereafter, sound pressure was propagated from the transmitter to the receiver. The water tank can be considered a reciprocal environment owing to its sufficiently larger dimension compared with the frequency. The FAA was located at the center of the water tank, and sound

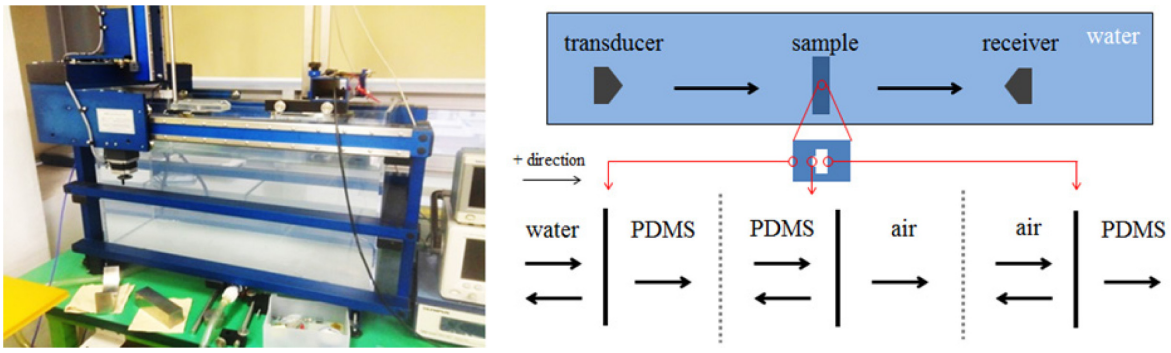

Fig. 3 Photography and schematic image of the attenuation experiment device

pressure at the receiver was converted into sound pressure level using the equation 20log P, where P is pressure.

3. Results and Discussion

The Helmholtz resonator consists of a neck and cavity. In this experiment, to form the neck and cavity, the Helmholtz resonator-inspired microstructure was fabricated through two-step photolithography. The microresonator shaped as a master was fabricated with a negative photoresist (SU-8, Microchem), whereas the polydimethylsiloxane (PDMS) resonator was fabricated through a simple molding process. The negative-tone micropatterns were arrayed with 184 μm period in a 40 × 40 mm square, and the samples consisted of PDMS, one of the well-known thermosetting polymers in the MEMS field. From the acoustics point of view, the acoustic impedance of sound wave is represented by the product of density and speed of sound in the medium. The difference in acoustic impedances plays an important role in the propagation and reflection of acoustic signals at the interface between dissimilar materials. If the difference between the acoustic impedances of two objects touching each other is small, the propagation of acoustic signals will proceed efficiently. On the contrary, if the difference is remarkably large, the acoustic signal will be reflected instead of being allowed to passing through. As the acoustic impedance of PDMS (0-1.04 Mrayl) is similar with that of water (0-1.5 Mrayl), PDMS was selected as the FAA material for observation of the attenuation effect. If a rigid polymer with significantly different impedance from water is used, the reflection characteristics of the sound itself will be measured rather than the characteristics of the resonating effect. In acoustics, simple analysis of the acoustic element can be achieved if the wavelength of sound wave in medium is remarkably longer than the dimensions of the acoustic device (Long Wavelength Approximation), which we consider a “lumped acoustic device.” Also, if an acoustic device is satisfied long wavelength approximation, specific morphologies of acoustic element are not important such as device shape, alignment, and so on. The resonant frequency of the Helmholtz resonator was considered as a lumped spring-mass system model and can be expressed as follows Eq. (1):

$$2\pi f = c \times \sqrt{\frac{S}{L'V}} \tag{1}$$

where f refers to the resonance frequency of the Helmholtz resonator, c denotes the sound speed in the medium, S represents the cross-sectional area of the neck, V corresponds to the internal volume of the resonator, and L' is the effective length of the neck with radius a. L' can be expressed as follows with respect to the flange: $L' = L + 1.7a$ (Flanged Outer End) and $L' = L + 1.4a$ (Unflanged Outer End).[7] Fig. 4(a) shows the schematic and photo/SEM images of FAA and the fabrication method. The entire fabrication process consisted of two-step photolithography, that is, molding and bonding, and the process yield was over 95%. Master mold production, which is the key to the success of FAA fabrication, was minimized by replicating the slave master with rigid polymers, such as polyurethaneacrylate (PUA), a UV-curable material for imprinting lithography. FAA was fabricated by bonding the molded negative-tone PDMS resonator-shaped array and supporting the PDMS sheet by plasma bonding. Under an incident acoustic signal, the fabricated FAA passes a part of the acoustic signal, whereas another portion of the signal is reflected by the resonance of the resonator array. As a result, a high sound pressure is observed on the side where the sound wave enters, and a low sound pressure is measured on the opposite side (Fig. 4(b)).

To measure the performance of the fabricated FAA and minimize the dissipation of acoustic signals, a measuring system, which includes a piezo transducer and a hydrophone (Fig. 4(c)), was set up inside a water bath. The fabricated FAA was fixed by a clamp between the transducer and hydrophone. As shown in Table 1, impedances of water and PDMS are similar enough to not need

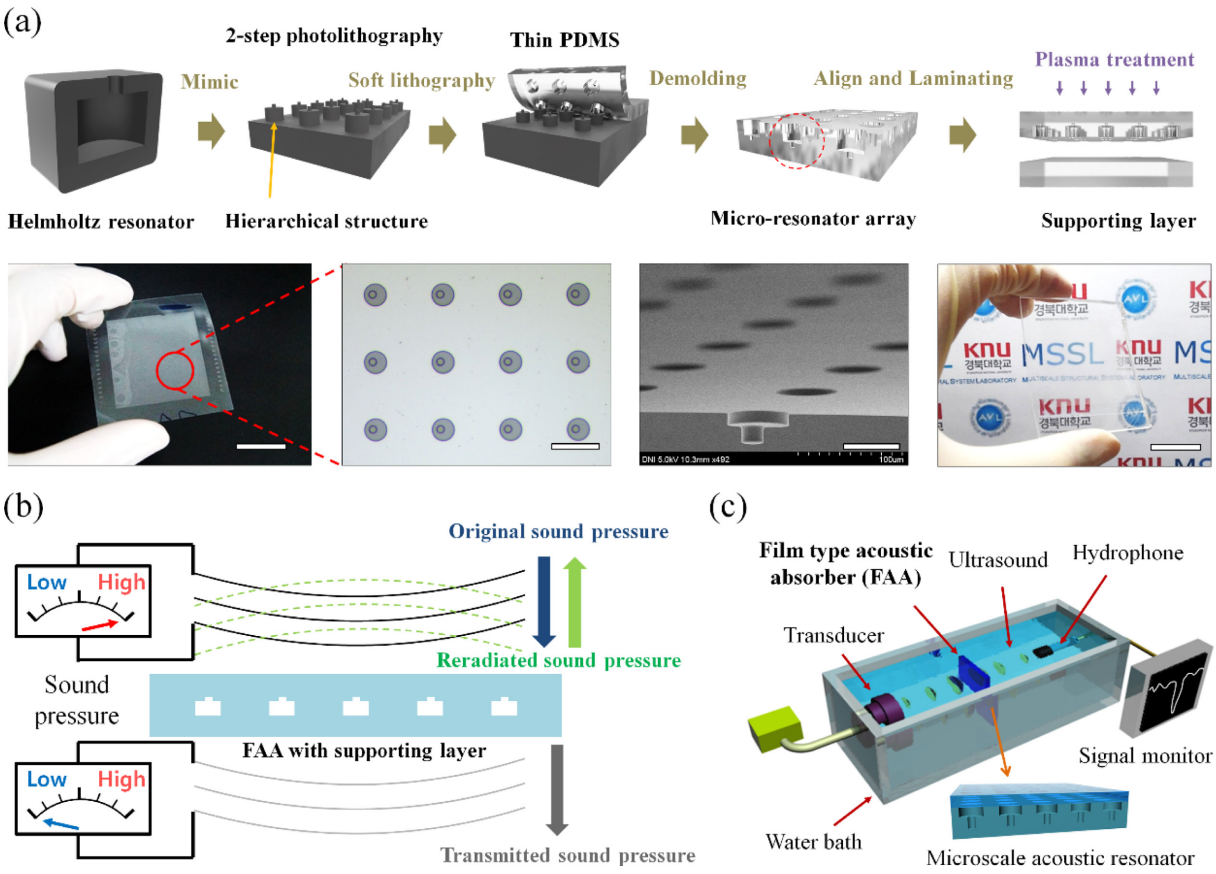

Fig. 4 Schematic and photo/scanning electron microscopy (SEM) images of the (a) Fabrication process of FAA inspired by the Helmholtz resonator. Scale bars are 2 cm, 100 and 50 μm, and 2 cm, respectively. (b) Acoustic attenuation principle of FAA and (c) Measurement system for the acoustic attenuation phenomenon

Table 1 Description of Impedance[21]

Property	Water	PDMS
Density (kg m^3)	1000	970
Speed of sound (m s^{-1})	1500	1080
Impedance (rayl)	1.5×10^6	1.04×10^6

any buffer layers during the experiments. Furthermore, as PDMS is hydrophobic and shows no swelling in water, it is a suitable material in this experiment. Simulation was conducted to predict the resonance phenomenon of the FAA. As shown in Fig. 5(a), an incident sound signal (0-1 MHz) was propagated on the FAA sample composed of PDMS, followed by the amplified sound pressure by the microscale resonator (0-60 μm) reradiating onto the incident sound pressure direction. Based on these results, we expected that reradiation of the acoustic signal due to resonance of the resonator will yield the same effect as attenuation due to interference and reduction of the transmitted acoustic signal. Furthermore, the FAA could be considered 'lumped acoustic deviced' since maximum length of unit element in the FAA (0-100 μm) is much smaller than the wavelength of the 1 MHz acoustic wave (0-1.5 mm) and could be applied 'long wavelength approximation'.

Prior to measurement of the attenuation performance of the fabricated FAA, a non-patterned PDMS sheet was first tested as the control sample.

The result for the control sample indicates that the attenuation value of the ultrasound signal is proportional to the input signal frequency, as shown by the green line (Reverse Triangle Symbol) in Fig. 5(b). This tendency is typically observed in common materials as the absorption coefficient is proportional to the square of the frequency. By contrast, in the case of the FAA sample, given a 60 μm cavity diameter, 12 μm cavity height, and 20 μm neck diameter, 19 μm neck height, the resonance frequency calculated for this sample is 0.88 MHz, and the actual measured maximum attenuation equals 1 MHz.

The maximum attenuation values for single, double, and triple layers reached 7, 9.5, and 12.8 dB mm^{-1}, respectively, at around 1 MHz. In every sample, the peak attenuation performance was observed at around the resonance frequency. From these

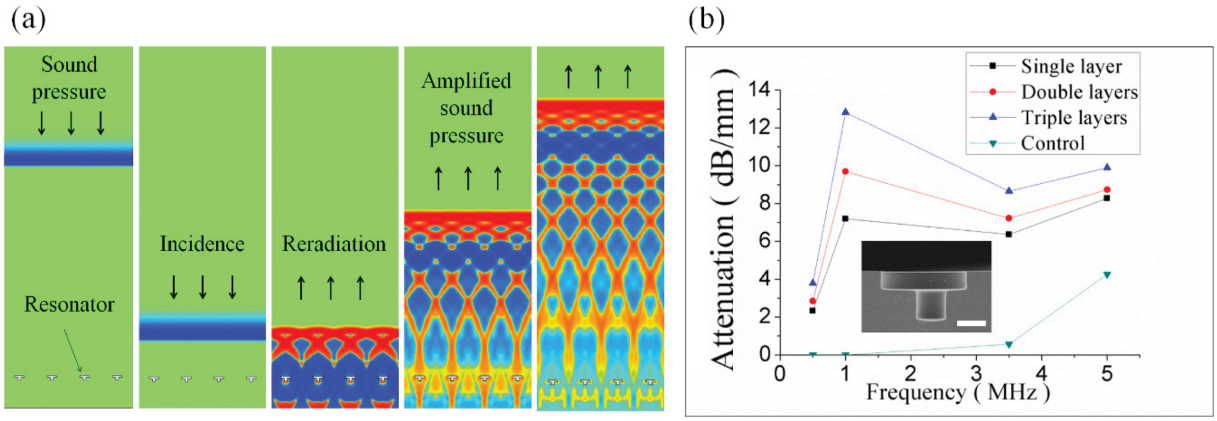

Fig. 5 (a) Simulation result of resonance in FAA. (b) Measured attenuation performances of FAAs with microscale resonators (Resonance frequency: 0.88 MHz) depending on input acoustic signal frequencies. The attenuation value of the non-patterned PDMS layer was measured as the control sample, and the values of the single, double, and triple layers of FAA were measured. Scale bar is 20 μm

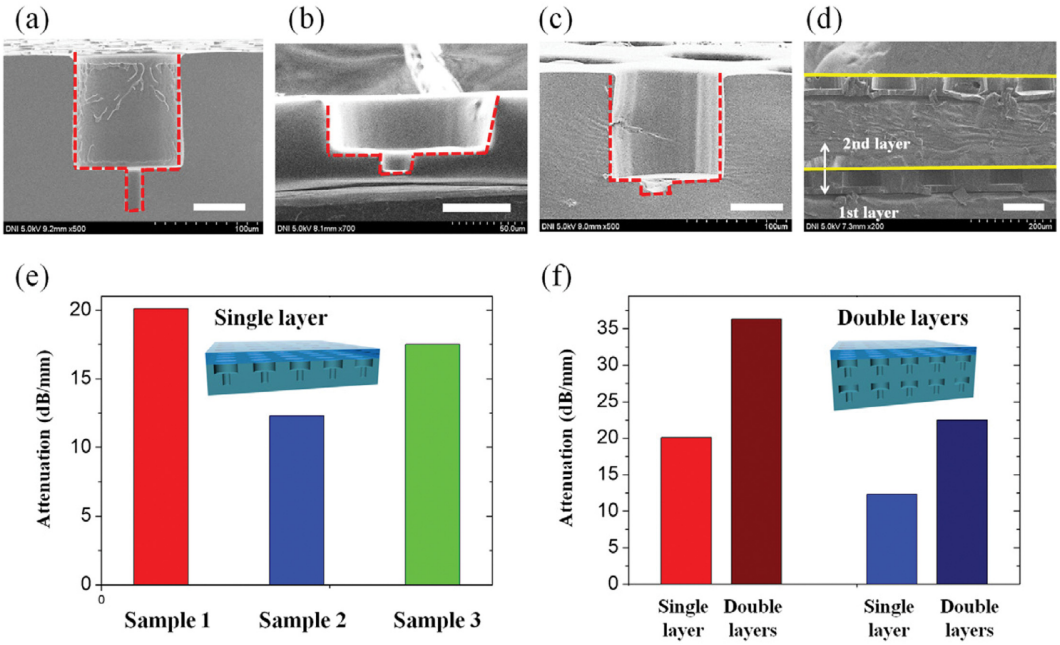

Fig. 6 SEM images of various FAAs. (a) Sample 1. (b) Sample 2. (c) Sample 3. (d) Double layers (Scale bars in (a)-(c) 50 μm; (d) 100 μm). (e) Attenuation data for three FAAs with various geometrical microscale resonators and (f) Attenuation data of the stacked absorbing sample by laminating two different resonator arrays (Samples 1 and 2).

attenuation values, the multiple FAA can enhance the attenuation value by stacking the layers; the attenuation is proportional to the number of laminated layers.

From the Eq. (1), we can predict that the resonance frequency of Helmholtz resonator can be controlled by changing the resonator dimensions. Although, the Eq. (1) is not applied in the FAA samples perfectly, to observe the influence of resonator dimension, various samples were fabricated, and the attenuation values were measured. To identify the relation of attenuation performance and resonator dimension, as shown in Figs. 6(a)-6(c), we measured the geometric values of various FAAs (Table 2).

Table 2. Geometric values of microresonator shown in Fig. 6(Cavity and neck diameters are fixed as 100 and 20 μm, respectively.)

	Cavity height (μm)	Neck height (μm)	Resonance frequency (kHz)
Sample 1	100	40	142
Sample 2	35	15	323
Sample 3	100	15	191

Fig. 6(e) indicates the comparison on performances of different geometric FAA samples. As shown in Table 2, three different

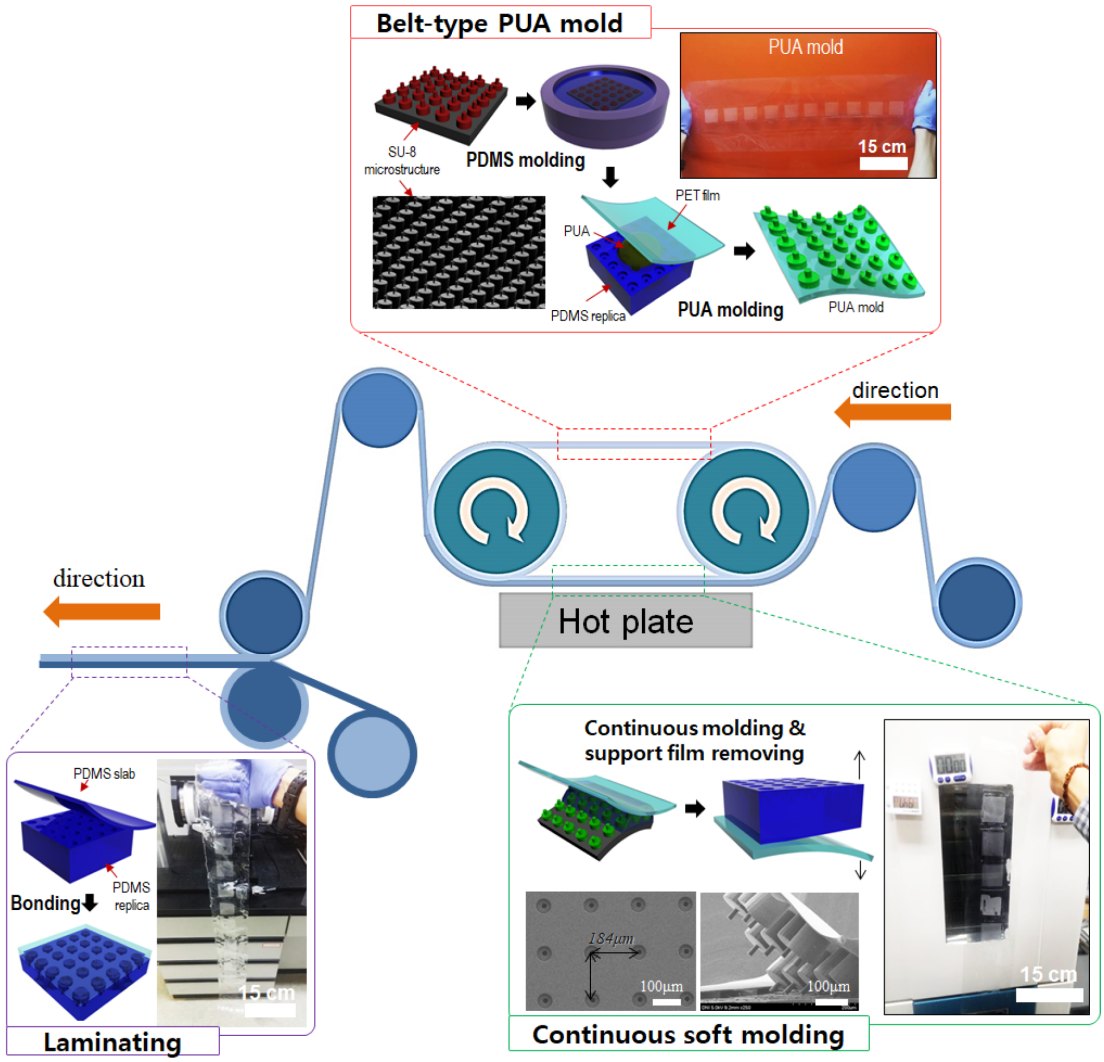

Fig. 7 Schematic description of the three parts of the roll-to-roll fabrication apparatus: belt-type PUA mold, continuous soft molding unit, and laminating unit. The belt-type PUA mold is wrapped around the pulleys of two neighbors. As heat is transmitted from the hot plate to the passing PDMS-coated substrate, the microscale resonator structures are continuously replicated on the feeding substrate

samples featured various cavity heights and neck lengths with the same diameters of cavity and neck. The single layer of Sample 1, which exhibited a 142 kHz resonance frequency, recorded the maximum attenuation value of 20.1 dB mm^{-1} at 1 MHz. To modulate the FAA performance, cavity volume was modulated by reducing the cavity height. The result indicates that the resonance frequency of Sample 2 changed to 323 kHz, and its maximum attenuation value was 12.1 dB mm^{-1} at 1 MHz. Given the similar resonance frequencies of these samples, their attenuation values at 1 MHz must be similar. However, the attenuation value of Sample 2 accounted for 59.8% of the result on Sample 1, resulting from the higher stiffness of Sample 2 than that of Sample 1. The stiffness of the Helmholtz resonator can be expressed as follows:

$$k = \frac{\rho c^2 S^2}{V} \quad (2)$$

where k refers to the stiffness of the Helmholtz resonator, c denotes the sound speed in the medium, ρ represents the density of the medium, S corresponds to the cross-sectional area of the neck, and V is the volume of the cavity. From the Eq. (2), k_1 (Stiffness of Sample 1) and k_2 (stiffness of Sample 2) were calculated at 1.7577 and 5.0221 mN m^{-1}, respectively. k_2 is three times higher than k_1. Therefore, decreasing cavity volume increases stiffness and decreases air displacement in the neck and cavity. This result indicates that a considerably high stiffness decreases the attenuation property of FAA. Such finding is attributed to the attenuation induced in the Helmholtz resonator by the elastic behavior of the PDMS microresonator and natural air-moving reaction between the air and neck. However, from a fabrication point of view, a long neck part, such as that of Sample 1, is difficult to fabricate with high yield and unsuitable for continuous fabrication. To secure high attenuation performance and

production yield, Sample 3 was produced with the same cavity as Sample 1 but with a shorter neck. In the results, Sample 3, with the same stiffness as Sample 1, recorded an attenuation of 17.5 dB mm^{-1} for a single-layer FAA. Consequently, a larger-sized cavity expressed higher attenuation performance due to the low stiffness of microscale resonators. In other words, geometrical values of resonators can be modulated for productivity without remarkable changing the attenuation performance.

As mentioned above, stacking the FAA layers enhances attenuation. Fig. 6(f) shows the attenuation performance of single-layer and double-layers FAAs, which have been fabricated by stacking different resonant FAAs (Samples 1 and 2), at 1 MHz (Fig. 6(d)). Both cases showed that the attenuation values of double-layer FAAs reached 36.3 and 22.5 dB mm^{-1}, which are 170 and 180% higher, respectively, than that of the single-layer ones (20.1 dB mm^{-1} for the single layer of Sample 1 and 12.3 dB mm^{-1} for the single layer of Sample 2). Especially, the double layer of Sample 1 achieved 36.3 dB mm^{-1} attenuation for 400 μm sample thickness; this value was recorded as the maximum attenuation in this study. Therefore, the fabricated FAA was measured with sufficient attenuation performance compared with typical acoustic absorbers.

To increase the productivity of the FAA, we have implemented continuous fabrication of FAAs by using custom-built roll-type equipment from our previous work.[15] Fig. 7 shows the schematics of the roll-to-roll fabrication system comprising a belt-type flexible PUA mold, hot plate, and motorized substrate feeding system. Using the master mold, the belt-type flexible PUA mold was produced via multiple lithography processes because the belt-type mold used in the roll-to-roll process should feature the same structure as the master mold on the flexible substrate.

After fabricating the flexible PUA mold, additional PDMS molding and laminating processes were performed to produce FAA samples continuously. As a result, we have achieved scalable fabrication of FAA via a continuous production system with fabrication speed of 100 mm min^{-1}.

4. Conclusions

In this study, Helmholtz resonator-inspired FAAs were produced by constructing arrays of microscale resonators. We observed that FAAs can absorb acoustic signal efficiently within the ultrasonic range, and the target frequency can be determined by modulating the geometric values of the resonator units. For enhancing productivity, FAA was fabricated via a roller-based continuous fabrication system. The fabricated FAAs exhibited several practical advantages, including high attenuation performance (0-36 dB mm^{-1}), easy production, controllability of resonance frequency, and potential in terms of broadened attenuation characteristics. With these developments, feasible applications will be sought in medical diagnosis equipment and military related devices through follow-up research.

ACKNOWLEDGEMENT

This work was supported by the National Research Foundation of Korea (No. NRF-2019R1A2C1086766) funded by the Korean Government (MSIT).

REFERENCES

1. Brunet, T., Merlin, A., Mascaro, B., Zimny, K., Leng, J., et al., “Soft 3D Acoustic Metamaterial with Negative Index,” Nature Materials, Vol. 14, No. 4, pp. 384-388, 2015.
2. Fang, N., Xi, D., Xu, J., Ambati, M., Srituravanich, W., et al., “Ultrasonic Metamaterials with Negative Modulus,” Nature Materials, Vol. 5, No. 6, pp. 452-456, 2006.
3. Khan, F.U., “Three Degree of Freedom Acoustic Energy Harvester Using Improved Helmholtz Resonator,” International Journal of Precision Engineering and Manufacturing, Vol. 19, No. 1, pp. 143-154, 2018.
4. Yoo, Y. J., Kim, Y. J., and Lee, Y., “Perfect Absorbers for Electromagnetic Wave, based on Metamaterials,” Journal of the Korean Physical Society, Vol. 67, No. 7, pp. 1095-1109, 2015.
5. Zhang, S., Yin, L., and Fang, N., “Focusing Ultrasound with an Acoustic Metamaterial Network,” Physical Review Letters, Vol. 102, No. 19, Paper No. 194301, 2009.
6. Zigoneanu, L., Popa, B. I., and Cummer, S. A., “Three-Dimensional Broadband Omnidirectional Acoustic Ground Cloak,” Nature Materials, Vol. 13, No. 4, pp. 352-355, 2014.
7. Kinsler, L. E., Frey, A. R., Coppens, A. B., and Sanders, J. V., “Fundamentals of Acoustics,” Fundamentals of Acoustics, 4th Ed., 1999.
8. Sugimoto, N. and Horioka, T., “Dispersion Characteristics of Sound Waves in a Tunnel with an Array of Helmholtz Resonators,” The Journal of the Acoustical Society of America, Vol. 97, No. 3, pp. 1446-1459, 1995.
9. De Bedout, J. M., Franchek, M. A., Bernhard, R. J., and Mongeau, L., “Adaptive-Passive Noise Control with Self-Tuning Helmholtz Resonators,” Journal of Sound and Vibration, Vol. 202, No. 1, pp. 109-123, 1997.
10. Wang, Z., Hu, Y., Meng, Z., and Ni, M., “Fiber-Optic Hydrophone Using a Cylindrical Helmholtz Resonator as a

Mechanical Anti-Aliasing Filter," Optics Letters, Vol. 33, No. 1, pp. 37-39, 2008.

11. Yasuda, T., Wu, C., Nakagawa, N., and Nagamura, K., "Studies on an Automobile Muffler with the Acoustic Characteristic of Low-Pass Filter and Helmholtz Resonator," Applied Acoustics, Vol. 74, No. 1, pp. 49-57, 2013.
12. Ahn, S. H. and Guo, L. J., "Large-Area Roll-to-Roll and Roll-to-Plate Nanoimprint Lithography: A Step toward High-Throughput Application of Continuous Nanoimprinting," ACS Nano, Vol. 3, No. 8, pp. 2304-2310, 2009.
13. Koo, S., Lee, S. H., Kim, J. D., Hong, J. G., Baac, H. W., et al., "Controlled Airbrush Coating of Polymer Resists in Roll-to-Roll Nanoimprinting with Regimented Residual Layer Thickness," International Journal of Precision Engineering and Manufacturing, Vol. 17, No. 7, pp. 943-947, 2016.
14. Kwak, M. K., Ok, J. G., Lee, S. H., and Guo, L. J., "Visually Tolerable Tiling (VTT) for Making a Large-Area Flexible Patterned Surface," Materials Horizons, Vol. 2, No. 1, pp. 86-90, 2015.
15. Lee, S. H., Kim, S. W., Kang, B. S., Chang, P. S., and Kwak, M. K., "Scalable and Continuous Fabrication of Bio-Inspired Dry Adhesives with a Thermosetting Polymer," Soft Matter, Vol. 14, No. 14, pp. 2586-2593, 2018.
16. Lee, S. H., Lee, J. H., Park, C., and Kwak, M. K., "Roll-Type Photolithography for Continuous Fabrication of Narrow Bus Wires," Journal of Micromechanics and Microengineering, Vol. 26, No. 11, Paper No. 115008, 2016.
17. Lee, S. H., Lee, J. H., Park, C. W., Lee, C. Y., Kim, K., et al., "Continuous Fabrication of Bio-Inspired Water Collecting Surface via Roll-Type Photolithography," International Journal of Precision Engineering and Manufacturing-Green Technology, Vol. 1, No. 2, pp. 119-124, 2014.
18. Lee, S. H., Kim, S. W., Park, C. W., Jeong, H. E., Ok, J. G., et al., "Scalable Fabrication of Flexible Transparent Heaters Comprising Continuously Created Metallic Micromesh Patterns Incorporated with Biomimetic Anti-Reflection Layers," International Journal of Precision Engineering and Manufacturing-Green Technology, Vol. 4, No. 2, pp. 177-181, 2017.
19. Ok, J. G., Kwak, M. K., Huard, C. M., Youn, H. S., and Guo, L. J., "Photo-Roll Lithography (PRL) for Continuous and Scalable Patterning with Application in Flexible Electronics," Advanced Materials, Vol. 25, No. 45, pp. 6554-6561, 2013.
20. Wi, J. S., Lee, S., Lee, S. H., Oh, D. K., Lee, K. T., et al., "Facile Three-Dimensional Nanoarchitecturing of Double-Bent Gold Strips on Roll-to-Roll Nanoimprinted Transparent Nanogratings for Flexible and Scalable Plasmonic Sensors," Nanoscale, Vol. 9, No. 4, pp. 1398-1402, 2017.
21. Tsou, J. K., Liu, J., Barakat, A. I., and Insana, M. F., "Role of Ultrasonic Shear Rate Estimation Errors in Assessing Inflammatory Response and Vascular Risk," Ultrasound in Medicine & Biology, Vol. 34, No. 6, pp. 963-972, 2008.

Sung Ho Lee
Postdoctoral researcher in the Department of Mechanical Engineering, Kyungpook National University. His research interest is micro/nano fabrication and its applications.
E-mail: lee_sh@knu.ac.kr

Jin Ho Choi
Senior Researcher in the Department of Mechanical Engineering, Kyungpook National University. His research interest is micro/nano fabrication and its applications.
E-mail: chlwlsgh01@gmail.com

Gyu Man Kim
Professor in the School of Mechanical Engineering, Kyungpook National University. His research interest is MEMS and its applications.
E-mail: gyuman.kim@knu.ac.kr

Yong Rae Roh
Professor in the School of Mechanical Engineering, Kyungpook National University. His research interest is Acoustic transducers and sensors.
E-mail: yryong@knu.ac.kr

Moon Kyu Kwak
Associate Professor in the School of Mechanical Engineering, Kyungpook National University. His research interest is Biomimetics and micro/nano continuous fabrication.
E-mail: mkkwak@knu.ac.kr